UNCLASSIFIED

Defense Technical Information Center
Compilation Part Notice

ADP013357

TITLE: On the GHz Frequency Response in Nanocrystalline FeXN Ultra-Soft Magnetic Films

DISTRIBUTION: Approved for public release, distribution unlimited

This paper is part of the following report:

TITLE: Materials Research Society Symposium Proceedings; Volume 720. Materials Issues for Tunable RF and Microwave Devices III Held in San Francisco, California on April 2-3, 2002

To order the complete compilation report, use: ADA410712

The component part is provided here to allow users access to individually authored sections of proceedings, annals, symposia, etc. However, the component should be considered within the context of the overall compilation report and not as a stand-alone technical report.

The following component part numbers comprise the compilation report:
ADP013342 thru ADP013370

UNCLASSIFIED

Mat. Res. Soc. Symp. Proc. Vol. 720 © 2002 Materials Research Society H3.14

On the GHz Frequency Response in Nanocrystalline FeXN Ultra-Soft Magnetic Films

N.G. Chechenin, C.B. Craus, A.R. Chezan, T. Vystavel, D.O. Boerma, J.Th. M. De Hosson and L. Niesen
Materials Science Centre, University of Groningen, Nijenborgh 4, NL-9747 AG Groningen, The Netherlands

ABSTRACT

The periodicity and angular spread of the in-plane magnetization for ultrasoft nanocrystalline FeZrN films were estimated from an analysis of the ripple structure, observed in Lorentz transmission electron microscopy (LTEM) images. The influence of the micromagnetic ripple on the ferromagnetic resonance (FMR) width is analyzed using an approach based on the Landau-Lifshitz equation. A strong dependence of the resonance width on the magnetic moment dispersion is predicted. To a large extent this particular aspect explains the high frequency response in some of our films.

INTRODUCTION

Nanocrystalline FeXN films proved to exibit excellent ultrasoft magnetic properties with a saturation magnetization up to or above $4\pi M \approx 15$ kG and a high magnetic susceptibility in the frequency range around and above 1 GHz [1-4]. The influence of the grain size, D, on the dc-magnetism has been analyzed in Hoffman's and Herzer's papers ([5,6] and ref. therein). A grain size much smaller than the size of the coupling volume is necessary to average out the magnetocrystalline anisotropy. The residual magnetocrystalline anisotropy, proportional to $D^{3/2}$, causes a stray field predominantly oriented along the easy axis and an angular spread of the magnetization, which is observed as a ripple structure in LTEM [7,8]. The amplitude of the angular spread β_0, which is a measure of the stray field, was obtained from an analysis of the LTEM ripples for the films deposited and post-treated under various conditions. The range of operating frequencies for these films is limited by the frequency and by the width of the FMR. Besides contributions to the FMR width due to dissipation sources, which are characteristic for crystalline and polycrystalline ferromagnetic films, an additional contribution exists in nanocrystalline films due tothe local variation of the magnetization. Despite of its importance, so far only few publications have addressed this problem.

Here we discuss the effect of the micromagnetic ripples on the FMR response, using an approach based on the Landau-Lifshitz equation where the effective field includes the internal stray field. We predict a strong dependence of the resonance width on the magnetic moment dispersion and show that the internal stray field can be a major cause of broadening of the FMR.

SAMPLE PREPARATION

Fe-Zr-N films were prepared by dc magnetron reactive sputtering. Films with a thickness between 50 and 1000 nm were deposited at several temperatures between room temperature and 200 °C. The films were grown in a nanocrystalline structural state on glass or silicon substrates. Polymer or Cu underlayers were used to be able to float the film on a grid for TEM investigation. The deposition conditions were chosen to obtain a composition $(Fe_{99}Zr_1)_{1-x}N_x$, where the concentration of nitrogen was in the range $x \leq 25$ at%. An 800 Oe magnetic field was applied in the plane of the samples during deposition. More details on the film deposition can be found in [9]. X-ray diffraction (XRD), as well as conventional TEM and selected area diffraction (SAD), reveal a 2-30 nm size of crystallites for most of the investigated sputter-deposited films, see, for example, Fig.1a.

LTEM ANALYSIS

The LTEM image in Figs. 1b, shows a ripple pattern, strongly dependent on the microstructure. For grain sizes of 10-50 nm and smooth, flat surfaces, the ripples are almost parallel (Fig.1a,b), while for films with a large roughness, grain size, porosity or other type of large size (>1μm) defects, the LTEM ripples start branching (Fig.1c,d) or form a disordered structure.

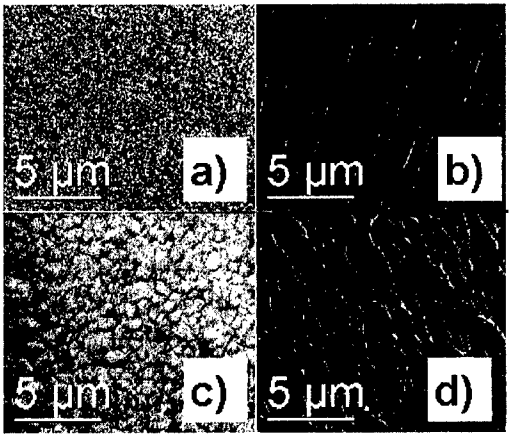

Figure 1. The ripples for two films with different microstructure.

It was noted [7] that, due to exchange interactions, longitudinal oscillations of the transversal component of the magnetization $\Delta M_y(x)$ are energetically more favorable than the transversal oscillations $\Delta M_y(y)$. Here the xy-plane is assumed to be parallel to the film surface and the x-axis parallel to the easy axis (EA). Approximating the oscillation by a single period harmonic function:

$$\Delta M_y(x) = M\beta_0 \sin(2\pi x/\lambda), \qquad (1)$$

one can relate, using the theory of electron diffraction, the contrast of the LTEM picture, C_x, with the periodicity, λ_x (in nm), of the ripples, with the deviation angle, β_0 (in degrees), of the local magnetization from the mean direction [10]

$$C_x = [Ix(0) - Ix(\lambda_x/2)]/Ix(\lambda_x/4) = = (4\pi M \beta_0 t \lambda_x / 2\Phi_0) \sin[\Delta z \lambda_0 / (2\pi \lambda_x^2)], \quad (2)$$

where $Ix(0)$, $Ix(\lambda_x/2)$ and $Ix(\lambda_x/4)$ are the image intensities in the maximum, in the minimum and in the middle point of the ripples, respectively, t is the thickness of the film (in nm), $\Phi_0 = h/2e$ is the flux quantum, Δz is the defocus distance in the microscope and λ_0 is the electron wavelength ($\lambda_0 = 2.5$ pm for the 200 keV- electrons). For maximum contrast one can obtain the relation, which has been used before [11]:

$$\beta_0 \approx 0.59 \times 10^5 C/(4\pi M t \lambda). \quad (3)$$

The periodicity in our films varies in a wide range from 200 nm to 2 μm, depending on the micro(magnetic) structure of the film. The uncertainty in the experimental values of λ and C was about ±20% and was due to a large variation in the distance between ripples, meaning that the ripples are not strictly periodic. Applying this analysis to different films, we obtained for β_0 values between 0.3^0 and 2.0^0. The β_0 values are $0.8^0 \pm 0.2^0$ and $1.5^0 \pm 0.3^0$ for the films shown in Fig.1a and 1c, respectively.

RF AND DC FIELD MEASUREMENTS

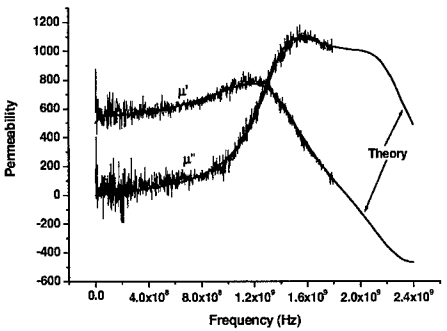

Figure 2. Frequency dependences $\mu'(f)$ and $\mu''(f)$. Experimental curves are fitted using (14) and (15) averaged over the period of the stray-field oscillations.

The technique for high frequency measurements was similar to that in [12]. The frequency dependences of the real, μ', and imaginary, μ'', parts of the permeability, plotted in Fig.2, correspond to the same sample as in Figs. 1a,b, i.e. for the sample with a polymer underlayer. The spectra were obtained in the absence of a dc-field and with the rf-field perpendicular to the easy direction (EA). The sample does not show the best RF properties we obtained, but allows a fair comparison between LTEM and RF data. The observation limit of the frequency response was $f = \omega/2\pi \approx 1.8$ GHz, which is lower than the resonance frequency $f_{00} = 1.9$ GHz, determined by zero-crossing of μ'. The $\mu''(f)$ dependence shows a bump at 1.6 GHz, i.e. at a significantly lower value than f_{00}.

THEORY

Let the local EA be at an angle β with the x-axis. The magnetization $\boldsymbol{M}$ is at an angle ϕ with the x-axis, at θ with the surface normal (z-axis) or at $\psi = 90^0 - \theta$ with the film surface. H_{dc} is the magnitude of the dc-magnetic field applied along the x-axis, H_{rf} is the high frequency the field applied along the hard axis direction. The Landau-Lifshiz equation reads:

$$d\boldsymbol{M}/dt = \gamma \boldsymbol{M} \times (-\nabla E) - (\alpha\gamma/M)\boldsymbol{M} \times [\boldsymbol{M} \times (-\nabla E)], \tag{4}$$

where α is a damping coefficient, γ is the gyromagnetic ratio, $-\nabla E$ is the generalized force. For the free energy we have

$$E = K\sin^2(\phi - \beta) - M\,[H_{dc}\cos\psi\cos\phi + H_{str}\cos\psi\cos(\phi - \phi_0) + H_{rf}M\cos\psi\sin\phi - (1/2)N_z M\sin^2\psi], \tag{5}$$

where K is the anisotropy constant, $N_z = 4\pi$ is the demagnetizing factor and ϕ_0 defines the local direction of $\boldsymbol{M}$, when only dc-field is applied. For a single-harmonic longitudinal oscillation of magnetization vector, Eq. (1), one can obtain for the stray field

$$H_{str,x} = -\pi M_0 \beta_{10}^2 \cos(4\pi x/\lambda), \tag{6}$$

Assuming $\alpha, \phi, \phi_0, \beta, \psi << 1$, $H_{str}, H_{dc}, H_k = 2K/M << M$, and $H_{rf} << H_{str}, H_{dc}, H_k$ one can obtain a linear differential equation:

$$d^2\phi/dt^2 + \alpha\gamma 2N_z M(d\phi/dt) + \omega_0^2\phi + \gamma^2\beta H_k = = (\gamma^2 N_z M + i\alpha\gamma\omega)H_{rf}\ , \tag{7}$$

where $\omega_0^2 = \gamma^2 N_z M(H_{eff} + H_{str})$ with $H_{eff} = H_{dc} + H_k$ (8)

If $H_{rf} = h_{rf}\exp(i\omega t)$, then a solution can be found in the form of

$$\phi = \phi_0 + \phi_1 \exp(i\omega t + i\delta), \tag{9}$$

Substituting $\phi(t)$ into the differential equation (7) gives

$$\begin{aligned} &\phi_0 = \beta H_k / H_{eff}, \\ &\phi_1 = \gamma^2 h_{rf} N_z M / [(\omega_0^2 - \omega^2)^2 + (\alpha\gamma\omega N_z M)^2]^{1/2}, \\ &tg\,\delta = \alpha\gamma\omega N_z M / (\omega_0^2 - \omega^2). \end{aligned} \tag{10}$$

When the dc-field is perpendicular and the rf field parallel to the EA similar expressions can be obtained. This case can be easily treated when $H_{dc} >> Hk$ and the angle ϕ is close to $\pi/2$, so $\eta = \pi/2 - \phi << 1$, for which the differential equation (7) is valid with $H_{eff} = H_{dc} - H_k$ in Eq. (8).

Note, that the local variation of the resonance frequency ω_0 in (8) can be large if the magnitude of the stray field is comparable with the anisotropy and dc fields. Within the approximations made, we can write

$$\omega_0^2 = \gamma^2 N_z M(H_{dc} + H_{str} \pm H_k), \tag{11}$$

where + and – correspond to dc-field parallel and perpendicular to the EA, respectively. When the amplitude of the local variation of the stray field does not exceed the effective field $H_{eff} = H_{dc} \pm H_k$ then the broadening of the FMR width due to the stray field can be estimated roughly as

$$<\Delta\omega_0^2> = \gamma^2 N_z M <H_{str}^2>^{1/2} = \pi\gamma^2 N_z M^2 \beta_0^2/(2)^{1/2} \tag{12}$$

Eq. (12) can only be used for a rough evaluation and the average HF-response from the whole sample must be taken into account for a more quantitative analysis. For the magnetic permeability we can write

$$\mu = 4\pi M(\phi - \phi_0)/H_{rf} + 1 = 4\pi M \phi_1 exp(i\delta)/h_{rf} + 1 \tag{13}$$

So, for the real and imaginary parts of the local permeability one obtains:

$$\mu' = \frac{4\pi \frac{M}{H_{eff}}[1 + \frac{H_{str}}{H_{eff}} - (\frac{\omega}{\omega_{00}})^2]}{[1 + \frac{H_{str}}{H_{eff}} - (\frac{\omega}{\omega_{00}})^2]^2 + \alpha^2 (\frac{\omega}{\omega_{00}})^2 \frac{N_z M}{H_{eff}}} \tag{14}$$

$$\mu'' = \frac{4\pi\alpha (\frac{\omega}{\omega_{00}})(N_z)^{1/2} (\frac{M}{H_{eff}})^{3/2}}{[1 + \frac{H_{str}}{H_{eff}} - (\frac{\omega}{\omega_{00}})^2]^2 + \alpha^2 (\frac{\omega}{\omega_{00}})^2 \frac{N_z M}{H_{eff}}} \tag{15}$$

where $\omega_{00} = \gamma[N_z M H_{eff}]^{1/2}$ is the resonance frequency when the stray field is absent and H_{str} varies from place to place , according to (6). The average of the permeability over the film volume is obtained by numerical integration.

The averaged theoretical dependencies $\mu'(f/f_{00})$ and $\mu''(f/f_{00})$ with f_{00}= 1.9 GHz are fitted to the experimental data in Fig.2, with H_{dc}=0 and H_k = 18 Oe as obtained from dc-measurements. An almost perfect fit was obtained with only slightly different parameters for the μ' (α=0.016, β_0=2.4^0, $4\pi M$ = 14 kG) and for μ'' (α=0.011, β_0=2.4^0, $4\pi M$= 14 kG). An increase of the α in the fitted expression depresses the bump in $\mu'(f)$, while a decrease of the β_0–value leads to a too sharp $\mu''(f)$ and to a shift of both, μ' and μ'' to a higher frequency region. It is important to note that the model perfectly reproduces the asymmetric shape of the $\mu''(f)$ with a maximum below the f_{00}-value.

However, in order to reproduce the f_{00}-value, the anisotropy field has to be assumed somewhat higher than it follows from dc-measurements. In the example discussed above this difference is about $H_i \approx 10$ Oe, assuming $H_{eff} = H_k + H_i$. In other cases the difference is small. A similar extra field was necessary to postulate to describe observations in [13]. The value β_0=2.4^0, obtained above is about 3 times higher than the value, obtained from LTEM patterns. The origin of the

increase of the anisotropy field and the large angle of the oscillation of the magnetization is not clear at this moment. We suppose that both items point to a more complex magnetic response of the spin system in the GHz-region, than was assumed in the theory. The dynamical response is more complicated for films, which have a stronger static ripple structure. In spite of this, the shape of $\mu'(f)$ and $\mu''(f)$ are well described because the theory operates with the reduced frequencies (f/f_{00}), reduced magnetization, M/H_{eff}, and reduced stray field H_{str}/H_{eff}, as follows from (14) and (15).

CONCLUSIONS

From the LTEM data, we obtained a large variation of the periodicity and dispersion angle of the micromagnetic ripple for films deposited on different substrates and under different conditions. A large dispersion angle correlates with a large FMR width in high frequency scans. These observations are in a good correspondence with the theoretical analysis, which shows a large effect of the internal stray field in nanocrystalline soft magnetic films on the FMR response.

ACKNOWLEDGMENTS

This work was supported by the Dutch Stichting Technische Wetenschappen (STW) and the Prioriteitsprogramma Materialenonderzoek (PPM).

REFERENCES

1. B. Viala, M.K. Minor, J.A. Barnard, *J. Appl. Phys*, **80** (1996) 3941
2. H.Y. Wang, E.Y. Yang, H.L. Bai, P. Wu, Y.Wang, F.F. Gong, *J. Phys.: Condens. Matter.* **9** (1997) 8443
3. S. Jin, W. Zhu, T.H. Tiefel, V. Korenivski, R.B. van Dover, and L.H. Chen, *J. Appl. Phys.*, **81** (1997) 4042
4. O. Shimizu, K. Nakanishi, S. Yoshida, *J. Appl. Phys.* **70** (1991) 6244
5. H. Hoffmann, *Thin Solid Films*, **58** (1979) 223
6. G. Herzer, *Scripta Metallurg. Materialia*, **33** (1995) 1741
7. H.W. Fuller and M. E. Hale, *J. Appl. Phys.*, **31**, (1960) 238, *ibid,* 31 (1960) 1699
8. D. Wohlleben, *J. Appl. Phys.* **38** (1967) 3341
9. A.R. Chezan , C.B. Craus, N.G. Chechenin, L. Niesen, and D. O. Boerma, *Physica Status Solidi (a)*, **189** (2002) 833
10. N.G. Chechenin et al, to be published
11. N.G. Chechenin, A.R. Chezan, C.B. Craus, T. Vystavel, D. O. Boerma, J.Th.M.De Hosson and L. Niesen, *J. Magn. Magn. Mater.*, **239** (2002) p. 180
12. V. Korenivski, R.B. van Dover, P.M. Mankiewich, Z.-X Ma, A.J. Becker, P.A. Polakos, and V.J. Fratello, *IEEE Trans. Magn.* **32** (1996) 4905
13. D. Spenato, A. Fessant, J. Gieraltowski, H. Le Gall, and C. Tannous, *J. Appl. Phys.*, **85** (1999) 6010